Available online at www.sciencedirect.com

SCIENCE DIRECT®

Biochimica et Biophysica Acta 1689 (2004) 162–173

BIOCHIMICA ET BIOPHYSICA ACTA

BBA

www.bba-direct.com

Impaired mitochondrial respiratory chain and bioenergetics during chagasic cardiomyopathy development

Galina Vyatkina[a], Vandanajay Bhatia[a], Arpad Gerstner[b], John Papaconstantinou[b], Nisha Garg[a,c,*]

[a] *Department of Microbiology and Immunology, University of Texas Medical Branch, 301 University Boulevard, Galveston, TX 77555, USA*

[b] *Department of Human Biological Chemistry and Genetics, University of Texas Medical Branch, 301 University Boulevard, Galveston, TX 77555, USA*

[c] *Department of Pathology, Center for Biodefense and Emerging Infectious Diseases, and Sealy Center for Vaccine Development, University of Texas Medical Branch, 301 University Boulevard, Galveston, TX 77555, USA*

Received 15 December 2003; received in revised form 11 March 2004; accepted 11 March 2004

Available online 2 April 2004

Abstract

In this study, we evaluated the activities of respiratory chain complexes and oxidative phosphorylation (OXPHOS) capacity of the heart to gain insights into the pathological significance of mitochondrial dysfunction in chagasic cardiomyopathy (CCM). In a murine model of *Trypanosoma cruzi* infection, biochemical and histochemical analysis of the cardiac mitochondria revealed deficiency of the respiratory chain complexes (CI–CV) in infected mice; the inhibition of CI activity was more pronounced in the acute infection phase, CIII was constitutively repressed throughout the infection and disease phase, and the CV defects appeared in chronic phase only. A substantial decline in cardiac mtDNA content (54–60%) and mitochondria-encoded transcripts (50–65%) with disease development indicated that the alterations in mtDNA contribute to the quantitative deficiencies in respiratory chain activity in chagasic hearts. The observations of a selective inhibition of redox-sensitive CI and CIII complexes that are also the site of free radical generation in mitochondria, and the decline in cardiac mtDNA content in infected mice, all support the free radical hypothesis of mitochondria dysfunction in CCM. Consequently, OXPHOS-mediated ATP synthesis capacity of the cardiac mitochondria in infected mice was substantially reduced (37–50%), suggesting an energy homeostasis in the affected tissue.

Keywords: *Trypanosoma cruzi*; Chagasic cardiomyopathy; Free radical; mtDNA content; Oxidative phosphorylation; Respiratory chain complex

1. Introduction

Chagas disease is a pathological process induced by human infections with the hemoflagellate protozoan *Trypanosoma cruzi* and is a major health problem in the southern parts of the American continent [1]. Among the most common manifestations of disease is the slow progression of myocarditis that might evolve into chagasic cardiomyopathy (CCM) signified by diffused inflammatory reactions, hypertrophy, and fibrosis leading to ventricular dilation and cardiac arrhythmia [2]. Most studies on the pathogenesis of Chagas' disease have postulated the crucial role of parasite persistence in the development of clinical disease [3]. Others have proposed that an autoimmune mechanism [4,5] independent from parasite persistence is involved in the development of pathogenic processes in chronic Chagas' disease. However, despite decades of research, limited information is available on the cellular and molecular mechanisms by which cardiovascular functions are adversely affected in *T. cruzi*-infected patients and experimental models.

Infection by *T. cruzi* generally induces proinflammatory cytokines (TNF-α, IL-1, and IL-6) that play an important role in modulating host resistance to parasite. The prime

Abbreviations: BN-PAGE, blue native-polyacrylamide gel electrophoresis; CCM, chronic chagasic myocardiopathy; CI, NADH-ubiquinone oxidoreductase; CII, succinate-ubiquinone oxidoreductase; CIII, ubiquinol-cytochrome *c* oxidoreductase; CII+CIII, succinate-cytochrome *c* oxidoreductase; CIV, cytochrome *c* oxidase; CV, F_1F_0 ATP synthase; OXPHOS, oxidative phosphorylation; RCC, respiratory chain complexes; ROS, reactive oxygen species

* Corresponding author. Department of Microbiology and Immunology, University of Texas Medical Branch, 301 University Boulevard, Galveston, TX 77555, USA. Tel.: +1-409-747-6865; fax: +1-409-747-6869.

E-mail address: nigarg@utmb.edu (N. Garg).

0925-4439/$ - see front matter © 2004 Elsevier B.V. All rights reserved.
doi:10.1016/j.bbadis.2004.03.005

mechanism via which inflammatory cytokines participate in control of parasitic infections is through the activation of cytotoxic agents, including reactive oxygen species (ROS) and nitrogen species (RNS) [6]. For example, TNF-α has been shown to be effective in controlling parasite burden [7] partly by enhancing the NO-dependent trypanocidal activity of the activated macrophages [8]. The susceptibility of trypanosomes to reactive species and the direct role of ROS in limiting *T. cruzi* replication and survival in infected cells and experimental animals have also been reported [9]. During the process of parasite destruction, the host cells protect themselves from inflammatory mediators and reactive species via the activation of a cascade of defense and repair mechanisms that ensure cell survival [10,11]. However, when exposed to excessive insult, host components (DNA, lipids, and proteins) may also be damaged, resulting in inhibition of a variety of physiological functions, eventually leading to cell death [12,13]. Of note is the role of TNF-α-mediated cytotoxic reactions in inducing pro-apoptotic reactions, cell death, and tissue damage in *T. cruzi*-infected murine hearts [14,15]. IL-1 and IL-6 have also been associated with alterations in endothelial cell functions in experimental and human CCM [16]. Further studies would identify the host cellular and organelle functions that are adversely affected by the inflammatory mediators and may be of pathological importance in cardiovascular homeostasis associated with CCM development.

The heart is highly dependent on mitochondria for the energy required for its contractile and other metabolic activities. Mitochondria represent 30% of the total volume of cardiomyocytes and provide ~ 90% of the cellular ATP energy through oxidative phosphorylation (OXPHOS). Interestingly, mitochondria are the targets of a variety of endogenous and exogenous insults, including the inflammatory mediators. The damage of mitochondrial membrane phospholipids, DNA, or proteins can have multiple effects on mitochondria function, including increased permeability of the mitochondrial membranes, loss of the mitochondrial components (e.g. cytochrome *c*), dissipation of the mitochondrial membrane potential and protonmotive force, and the decreased activity of the respiratory chain complexes (RCC, CI–CV) [17–19]. The eventual outcome of mitochondrial abnormalities is the impairment of the OXPHOS capacity, which is likely to have an adverse influence on energy production and cardiac performance.

Recently, we demonstrated in a murine model of *T. cruzi* infection and disease development, the accumulation of irregular and swollen mitochondria that may also be dysfunctional [20]. The repression of a variety of transcripts encoding components of the respiratory complexes suggested that chagasic hearts might be compromised in their respiratory activity [20]. In this study, we sought to determine (i) whether the activities of the respiratory complexes is impaired during progressive cardiomyopathy in a murine model of *T. cruzi* infection and disease development, and (ii) if the mitochondrial respiratory chain defects disturb the cardiac energy status in infected mice? Our results support a relationship between depletion of the mtDNA content and expression, the loss in RCC activities, and the decline in OXPHOS capacity with disease severity in infected murine hearts. We discuss the potential contribution of CI and CIII deficiencies in promoting free radical production and mitochondrial dysfunction in CCM.

2. Materials and methods

2.1. Mice and parasites

Six- to eight-week-old male C3H/HeN mice (Harlan Labs) were used in all experiments. The SylvioX10/4 strain of *T. cruzi* and C2C12 cells (murine skeletal muscle hybridoma cells) were purchased from American Tissue Culture Collection (ATCC, Rockville, MD). *T. cruzi* trypomastigotes were maintained and propagated by continuous in vitro passage in C2C12 cells [21]. Mice were infected by intraperitoneal injection of 50,000 culture-derived trypomastigotes. Animal experiments were performed according to the National Institutes of Health Guide for Care and Use of Experimental Animals and approved by the UTMB Animal Care and Use Committee.

2.2. Biochemical measurements

The myocardial content of DNA, RNA, and protein was measured at different stages of infection and disease development and expressed as mg/g wet weight [22].

2.3. Isolation of mitochondria

Mice were sacrificed during the immediate early (3–10 days post-infection, dpi), acute (15–40 dpi), and chronic (>110 dpi) phases of infection and disease development. Samples of heart ventricle and skeletal muscle were washed and suspended in ice-cold isolation buffer (5 mM HEPES, pH 7.2 containing 210 mM mannitol, 70 mM sucrose, 1 mM EGTA, and 0.5% BSA (fatty acid-free), tissue/buffer ratio, 1:10 w/v) and immediately homogenized [20]. Homogenates were centrifuged at 1000 × *g*, 4 °C for 5 min and the supernatant transferred to a new tube. The pellet was re-suspended in isolation buffer, homogenized, and centrifuged again as described above. The combined supernatants were centrifuged at 8100 × *g* for 15 min at 4 °C, the mitochondrial pellet re-suspended in isolation buffer (tissue/buffer, 1:1 ratio, w/v), and the aliquots stored at − 80 °C. Protein concentrations were determined by the Bradford method [23].

2.4. Spectrophotometric evaluation of the RCC activities

The measurement of the specific activity of the RCC was performed as described [24,25] with slight modifications. All

assays were performed in 1 ml final volume with 5–10 μg mitochondrial proteins, and the linear change in absorbance measured for 3 min. CI (NADH-ubiquinone oxidoreductase): the reaction mixture consisted of 10 mM Tris–HCl pH 8.0 buffer, 80 μM 2,3-dimethoxy-5-methyl-6-decyl-1, 4-benzoquinone (DB), 1 mg/ml BSA, 0.25 mM KCN, and 0.4 μM antimycin. After incubating mitochondria in the reaction mixture at 30 °C for 5 min, oxidation of NADH (200 μM) was monitored at 340 nm (ε5.5 mM^{-1} cm^{-1}). CII (succinate-ubiquinone oxidoreductase): mitochondria were incubated in 50 mM potassium phosphate buffer pH 7.4 containing 20 μM succinate. After addition of assay mixture consisting of 50 μM 2,6-dichlorophenolindophenol (DCPIP), 2 mM KCN, 2 μg/ml rotenone, 2 μg/ml antimycin; 25 μM DB was mixed. The reduction of DCPIP in association with CII-catalyzed DB reduction was measured at 600 nm (ε19.1 mM^{-1} cm^{-1}). CIII (ubiquinol-cytochrome *c* oxidoreductase): mitochondria were suspended in 50 mM Tris–HCl buffer, pH 7.4 containing 1 mM EDTA, 250 mM sucrose, 2 mM KCN, and 50 μM oxidized cytochrome *c*. After the addition of 80 μM reduced DB (DBH_2), reduction of cytochrome *c* was measured at 550 nm (ε19.0 mM^{-1} cm^{-1}). CII + CIII (succinate-cytochrome *c* oxidoreductase): mitochondria were incubated in 40 mM potassium phosphate buffer pH 7.4, 20 mM succinate, 0.5 mM EDTA, 2 mM KCN, and 30 μM cytochrome *c*. The reduction of cytochrome *c* by CIII coupled to oxidation of succinate through CII reaction was measured at 550 nm (ε19.0 mM^{-1} cm^{-1}). CIV (cytochrome *c* oxidase): mitochondria (2 μg protein) were permeabilized in 10 mM Tris–HCl pH 7.0, 25 mM sucrose, 120 mM KCl, and 0.025% *n*-dodecyl-β-D-maltoside, and 50 μM reduced cytochrome *c* added. The oxidation of cytochrome *c* was measured at 550 nm (ε19.0 mM^{-1} cm^{-1}). Citrate synthase: mitochondria were added to 100 mM Tris–HCl buffer pH 8, 0.3 mM acetyl CoA, 100 μM 5,5′-dithio-bis 2-nitrobenoic acid (DTNB). The reaction was initiated by 0.5 mM oxaloacetate. Citrate synthase-catalyzed reduction of acetyl CoA with oxaloacetate in conjunction with DTNB reduction was monitored at 412 nm (ε13.6 mM^{-1} cm^{-1}). Specificity of the respiratory complexes activities was determined by monitoring changes in absorbance in the presence of the specific inhibitors: CI (rotenone, 6.5 μM), CII (sodium malonate, 10 mM), CIII (antimycin, 5 μg/ml), and CIV (KCN, 1 mM).

2.5. Blue native-polyacrylamide gel electrophoresis (BN-PAGE) and histochemical staining

Mitochondria for BN-PAGE were isolated in 20 mM Tris–HCl pH 7.4, 250 mM sucrose, 2 mM K_2EGTA. Mitochondrial pellets (500 μg protein) were suspended in 60 μl extraction buffer (50 mM imidazole pH 7.0, 5 mM aminocaproic acid, 50 mM NaCl) containing protease inhibitor cocktail [20] and the mitochondrial membranes were solubilized by adding 6 μl of freshly prepared 10% dodecyl maltoside (protein/detergent ratio, 1:6) [26]. Following incubation on ice for 30 min, samples were centrifuged at 13,000 × *g*, 4 °C for 15 min. The supernatants (70 μl) were transferred to a clean tube, and 3.5 μl of 5% Coomassie brilliant blue G-250 suspension in 0.5 M aminocaproic acid, 10% glycerol (Coomassie/detergent ratio, 1:4) added. A 5–12% polyacrylamide gradient gel with 4% stacker gel for electrophoresis was poured into a BioRad mini-gel apparatus and samples loaded immediately. Electrophoresis was run at 4 °C, 15 min each at 125 and 250 V using separate anode (25 mM imidazole HCl pH 7.0) and cathode (50 mM Tricine, 7.5 mM imidazole, pH 7.0, 0.02% Coomassie G-250) buffers. After 30 min, cathode buffer without Coomassie G-250 was added and electrophoresis continued at 250 V for 40 min [26].

Catalytic staining reactions to evaluate the activity of the respiratory complexes were performed immediately after the first dimension BN-PAGE [27,28]. Briefly, CI activity was determined by incubation of the gel slices with 1 mM Tris–HCl, pH 7.4, 0.1 mg/ml NADH, and 2.5 mg/ml nitrobluetetrazolium at room temperature. For the detection of CII activity, gel slices were incubated with 1.5 mM phosphate buffer pH 7.4 containing 5 mM EDTA, 10 mM KCN, 0.2 mM phenazine methosulfate, 84 mM succinate, and 10 mM nitrobluetetrazolium. CIV activity was estimated by incubating the gel slices in dark with 50 mM phosphate buffer pH 7.4, 0.5 mg/ml 3,3′-diaminobenzidine tetrahydrochloride, 75 mg/ml sucrose, 2 μg/ml catalase, and 1 mg/ml reduced cytochrome *c*. To obtain the CV (F_1F_0 ATP synthase) activity, gel slices were incubated in dark in 35 mM Tris–HCl pH 7.8 containing 270 mM glycine, 14 mM $MgSO_4$, 0.2% $Pb(NO_3)_2$, and 8 mM ATP. For the preservation of the color of CI-, CII-, and CIV-reacting bands, gel slices were fixed in 50% methanol, and 10% acetic acid, and stored in 10% acetic acid. The white–black color of CV was visualized and photographed immediately. Densitometric quantitation of all colored bands was performed on a FluorChem 8800 (Alpha Innotech) image-analyzing system.

2.6. mtDNA content

The mtDNA content in infected murine hearts was examined by Southern blot analysis. Cardiac tissue samples were homogenized in 10 mM Tris HCl, pH 7.5, 10 mM EDTA, 0.1 M NaCl, and proteins in tissue lysates digested by incubation overnight at 55 °C in the presence of 0.5% SDS, 20 μg/ml Proteinase K. After digestion of the cellular RNA with 5 μg/ml RNase A for 1 h at 37 °C, samples were extracted twice with phenol/chloroform/isoamylalcohol (24:24:1) and DNA purified by ethanol precipitation. DNA was digested with *Nco*I or *Bam*HI restriction enzymes, separated on 0.8% agarose gel, and transferred to zeta probe membrane (Bio-Rad). The [^{32}P]-labeled *COX2* and *β-actin* cDNA probes were generated by random primer labeling in the presence of 5 μl of [α^{32}P] dATP (3000 μCi/mmol, 10 μCi/μl, Amersham, Piscataway, NJ). The membranes were hybridized with *COX2* probe at 60 °C overnight, washed, exposed to a phosphorimaging screen, and the images captured using a

Storm 860 phosphorimager (Molecular Dynamics, Sunnyvale, CA). After stripping of the *COX2* probe, same membranes were hybridized with *β-actin* probe. The band intensities were compared by densitometric analysis.

2.7. Mitochondria-encoded gene expression

We examined mitochondria-encoded gene expression by Northern blotting. Total RNA from cardiac tissue samples was extracted by acid guanidinium-thiocyanate method [29] with slight modifications [20]. Samples (5 μg total RNA) were denatured in 50% formamide/2 M formaldehyde, electrophoresed in 1% agarose gel containing 2 M formaldehyde in 4-morpholinepropanesulfonic acid (MOPS) buffer and transferred to zeta probe membrane. The membranes were hybridized with [^{32}P]-labeled cDNA probes at 42 °C for 24 h followed by washing in 0.1 × SSC with 0.1% SDS at 55 °C. After exposure to a phosphorimaging screen, images were captured as above. All cDNAs used as probe for Southern and Northern blotting were amplified by RT-PCR using gene-specific primer pairs (listed in Table 1) with total RNA isolated from C57BL/6 mouse as template. The cDNA amplicons were cloned in Topo (T) vector, and confirmed by restriction digestion and sequencing at the Recombinant DNA Core Facility at UTMB.

2.8. Mitochondrial ATP production rate

Freshly harvested cardiac tissue samples were homogenized in 50 mM Tris pH 7.2 containing 100 mM KCl, 5 mM $MgCl_2$, 1.8 mM ATP, 1.0 mM EDTA and mitochondria isolated as above. The ATP production capacity of the freshly isolated mitochondria was monitored by a firefly luciferase method [30] using a TD-20/20 Luminometer (Turner Designs, Sunnyvale, CA). Briefly, 800 μl of ATP monitoring reagent consisting of 15 mM potassium phosphate pH 7.0, 150 mM sucrose, 2 mM $MgAc_2$, 0.5 mM EDTA, 2.5 μg/ml luciferase, 20 μg/ml D-luciferine, and 0.5 mg/ml BSA was aliquoted in 1 ml cuvettes. After 5 min incubation, 50 μl mitochondria (~ 100 μg tissue weight, 3–5 μg protein) and 50 μl 12.5 mM ADP was added and the assay monitored for 5 min in the presence of one of the following substrate combinations: 15 mM glutamate + 15 mM succinate; 30 mM glutamate + 20 mM malate; 31.5 mM TMPD + 7 mM ascorbate; 2.5 mM succinate + 2 mg/l rotenone; and 2.5 mM succinate. All assays were monitored in triplicate samples, and the results are presented as nmol ATP/min/mg wet tissue weight.

2.9. Statistical analysis

Qualitative data are expressed as raw data or percentages and compared using chi-square tests. Quantitative data is presented as mean ± S.D. The Student–Newman–Kreuls test was used for statistical evaluation of mean values for experimental and control animals. The level of significance were taken as $P < 0.05$.

3. Results

3.1. Impairment of the RCC activities in the myocardium of T. cruzi-infected mice

Previously, we demonstrated that C3H/HeN mice infected with the SylvioX10/4 strain of *T. cruzi* mimic the symptoms of human disease and provide an excellent experimental model for understanding the pathogenesis of progressive CCM. The course of disease development in these mice is divided into immediate early phase (3–5 dpi) of parasite invasion and initiation of innate inflammatory responses, acute phase (20–45 dpi) of parasite replication and activation of adaptive immune responses, followed by the progressive disease phase (>110 dpi) marked by minimal parasite burden,

Table 1
Genes analyzed in this study by Southern or Northern blotting

Gene Name	Product	GenBank Accession #	ORF (bp)	Forward primer (5′ → 3′)	Reverse primer (5′ → 3′)	Amplicon (bp)
Mitochondria-encoded genes						
Cytb	cytochrome *b*	V00711	1143	gttcgcagtcatagccacag	ggcggaatattaggcttcgt	596
AP6	ATP synthase subunit 6	V00711	681	ggattcccaatcgttgtagc	gggtgaatacgtaggcttgaa	601
AP8	ATP synthase subunit 8	V00711	204	tcatcacaaacattcccactg	ggggtaatgaatgaggcaaa	112
ND5	NADH oxidoreductase subunit 5	V00711	1824	tcctactggtccgattccac	aatgctaggcgtttgattgg	604
ND2	NADH oxidoreductase subunit 2	V00711	1038	cctatcacccttgccatcat	tgagggatgggttgtaagga	595
ND1	NADH oxidoreductase subunit 1	V00711	948	tcccctaccaataccacacc	acggaagcgtggataagatg	583
ND4L	NADH oxidoreductase subunit 4L	V00711	294	tgccatctaccttcttcaacc	tttggacgtaatctgttccgta	270
COX1	cytochrome *c* oxidase subunit 1	V00711	1545	ggtcaaccaggtgcactttt	ggtgcccaaagaatcagaac	598
COX2	cytochrome *c* oxidase subunit 2	V00711	684	atggcctacccattccaact	ttcagagcattggccataga	594
Nuclear encoded genes						
β-Actin	cytoplasmic β-Actin	M12481	1050	ccagatcatgtttgag	gtccagacgcaggatg	170
GAPDH	glyceraldehyde phosphate dehydrogenase	M32599	1228	tggcaaagtggagattgttg	ttcagctctgggatgacctt	600

ORF: open reading frame.

diffused inflammation and cellular fibrosis, and tissue degeneration in the myocardium [20]. The accumulation of irregular and swollen mitochondria and repression of transcripts for subunits of the respiratory complexes with progressive disease development [20] suggested that the activity of the RCC might be compromised in the myocardium of infected mice. To determine if such is the case, we evaluated the enzymatic activities of the respiratory complexes in the myocardium of infected mice.

We observed a substantial decline in the activity of the selective respiratory complexes in the myocardium of infected mice during disease progression (Fig. 1). CI exhibited earliest and strongest repression in response to *T. cruzi* infection; we observed a 38% loss in CI activity at 3 dpi and a 47–57% decline during 25–40 dpi relative to controls. With control of acute parasitemia, however, CI activity was recovered substantially, even though statistically significant loss in activity (~ 18%, $P>0.05$) persisted throughout the disease phase (Fig. 1). CIII specific activity diminished in infected murine hearts throughout the infection and disease phase; a 39–42% decrease in activity was observed during the acute phase, while 52–60% loss in CIII activity persisted during the chronic disease phase (Fig. 1). Similar to CIII, infected murine hearts exhibited a decrease (23–42%) in coupled CII + CIII activity during the entire course of infection and disease development. It should be noted that in normal mitochondria, CII catalyzes the rate-limiting step in a coupled CII + CIII assay [31,32]. In our experiments, we did not observe any alterations in CII activity (Fig. 1), thus suggesting that severe inhibition of CIII might contribute to overall decline in coupled CII + CIII activity. CIV appeared to be most resistant to *T. cruzi*-induced changes; we observed a 14–36% decline in CIV activity in infected murine hearts as compared to controls. In late chronic phase (180 dpi), CIV activity was restored to the levels similar to that detected in control mice (Fig. 1). Similar levels of CII activity in all cardiac mitochondria samples extracted from infected and normal tissues confirm the comparable efficiency of mitochondria isolation in different experiments (Fig. 1). In skeletal muscle mitochondria of infected mice, except for a decline in CI activity (40% inhibition), we observed no statistically significant impairment of CII, CIII, and coupled CII + CIII activities at all stages of infection and disease progression (unpublished observations).

3.2. Histochemical staining confirmed the RCC dysfunction in chagasic myocardium

One limitation with the estimation of enzymatic activities by spectrophotometric method in tissue homogenates and partially purified mitochondria is the detection of cellular activities that may not be specific to mitochondrial respiratory complexes. To overcome this limitation, we performed BN-PAGE analysis and quantitated the activities of the RCC by catalytic staining followed by densitometric analysis. To correct for the differences in loading of the

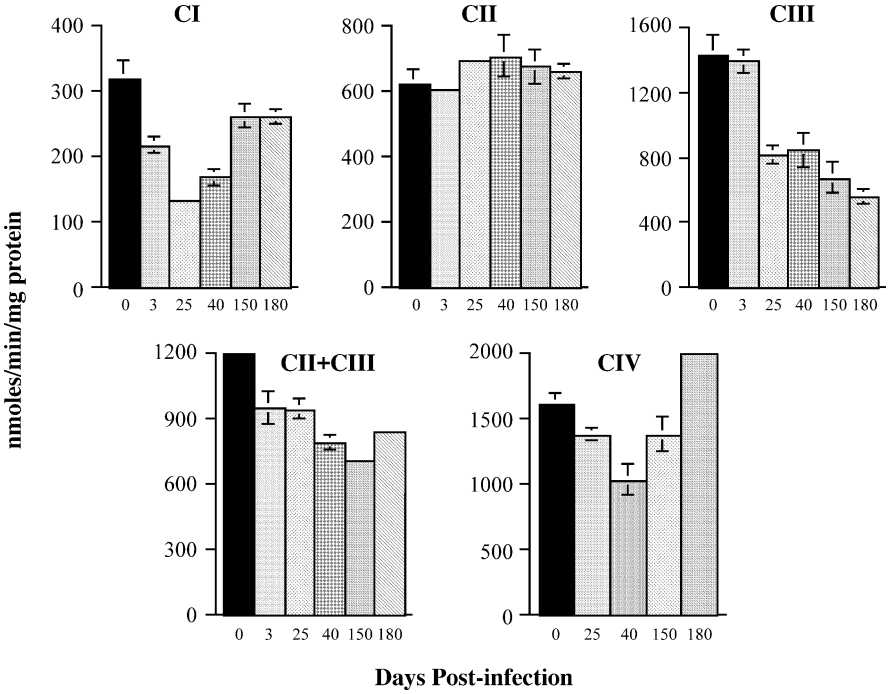

Fig. 1. Deficiency of respiratory complexes in the myocardium of *T. cruzi*-infected mice. C3H/HeN mice were infected by intraperitoneal injection with *T. cruzi* (SylvioX10/4 strain, 50,000 parasites/mouse). The activities of respiratory complexes CI–CIV and coupled CII + CIII activity were measured in cardiac mitochondria isolated from normal mice and *T. cruzi*-infected mice sacrificed at various time-points post-infection. The complexes activity was monitored by the oxidation of NADH (CI) and cytochrome *c* (CIV), and the reduction of DCPIP (CII) and cytochrome *c* (CIII and CII + CIII) (details in Materials and methods). Specific activity (nmol/min/mg protein) was calculated as mean ± S.D. obtained from duplicates estimated in three independent experiments.

protein complexes, the area of each complex from catalytic staining was expressed relative to the Coomassie-stained complex (Fig. 2).

Histochemical staining of BN gels provided evidence for the loss of respiratory complex activities with progressive disease development in the myocardium of infected mice (Fig. 2). Interestingly, catalytic staining revealed a >50% reduction in CI activity during the acute phase and recovery of CI activity after the acute infection phase. However, there was a significant difference in the extent of improvement; the spectrophotometric estimations of CI activity suggested up to 40% recovery of the CI activity in chronically infected murine hearts (150–180 dpi) as compared to that measured during the acute phase (25–40 dpi), whereas catalytic staining indicated that only 20% of CI activity was retrieved in chronically infected mice (Fig. 1 versus Fig. 2A,C). These discrepancies could be due to differences in extraction procedures and the sensitivity of the measurement method. However, given that the spectrophotometric assay detects other cellular activities, while BN-PAGE specifically measures the OXPHOS enzyme, it is likely that the latter is a more reliable measurement of CI activity. The histochemical changes in the specific activity of CIV at different stages of infection and disease progression were similar to that detected by spectrophotometric methods, while no change in CII activity was observed during the entire course of infection and disease development (data not shown). Catalytic staining for CIII failed to provide reproducible results with normal murine tissues and is, therefore, not included in the study. Interestingly, acutely infected mice exhibited an increase in CV activity (14–30%) when a substantial loss in the activity of other respiratory complexes was noted (Fig. 2A and C). However, with progressive disease development, >30% loss in CV activity was observed in the myocardium of infected mice relative to normal controls (Fig. 2A and C). Together, spectrophotometric and histochemical staining assays confirm the deficiencies of RCC in response to *T. cruzi* infection in murine myocardium.

3.3. Aberrations in mtDNA content and mitochondria-encoded gene expression in chagasic mice

A loss in mitochondrial respiratory complexes activities is often caused by damage of the mtDNA and/or changes in the expression of mitochondria-encoded subunits of the respiratory complexes. To determine if mtDNA is altered with disease progression, we estimated mtDNA content in infected murine hearts at various stages of disease development. Southern blot analysis was performed using mtDNA-specific *COX2* probe and nuclear DNA (nDNA)-specific *β-actin* probe and the intensity of the 7 and 16 kb mtDNA bands recognized by *COX2* probe (Fig. 3A) and 2 kb nDNA band recognized by *β-actin* probe (Fig. 3B) estimated by densitometric analysis. mtDNA content in normal and

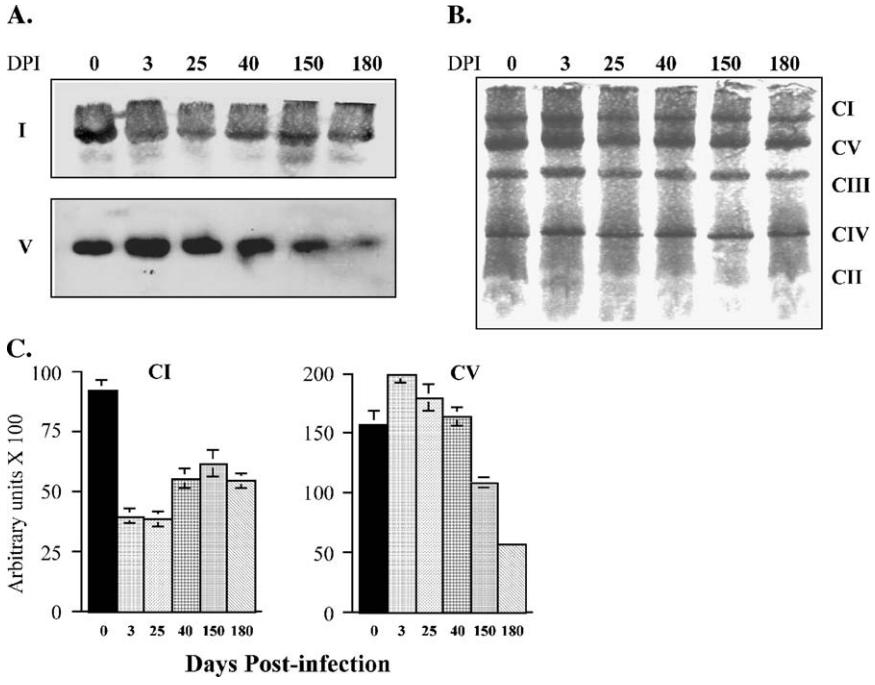

Fig. 2. Histochemical staining of blue-native gels confirms the loss of CI and CV activities in cardiac tissue of *T. cruzi*-infected mice. Mitochondria from cardiac tissue of normal and *T. cruzi*-infected mice sacrificed at 3, 25, 40, 150, and 180 dpi were isolated by differential centrifugation. The CI-CV complexes in the mitochondria preparations were resolved by BN-PAGE. The BN gels were either stained with Coomassie blue (panel B) or gel slices containing individual complexes were subjected to enzymatic colorimetric reactions (panel A) as described in Materials and methods. (C) Quantitation of the activity of the respiratory complexes. The histochemically stained and Coomassie blue-stained areas of the RCC were evaluated by densitometric analysis. Quantitative data were estimated as the ratio between the arbitrary units obtained for catalytic stained complex and the corresponding Coomassie stained complex × 100. The data present mean values obtained from at least three independent experiments. DPI, days post-infection.

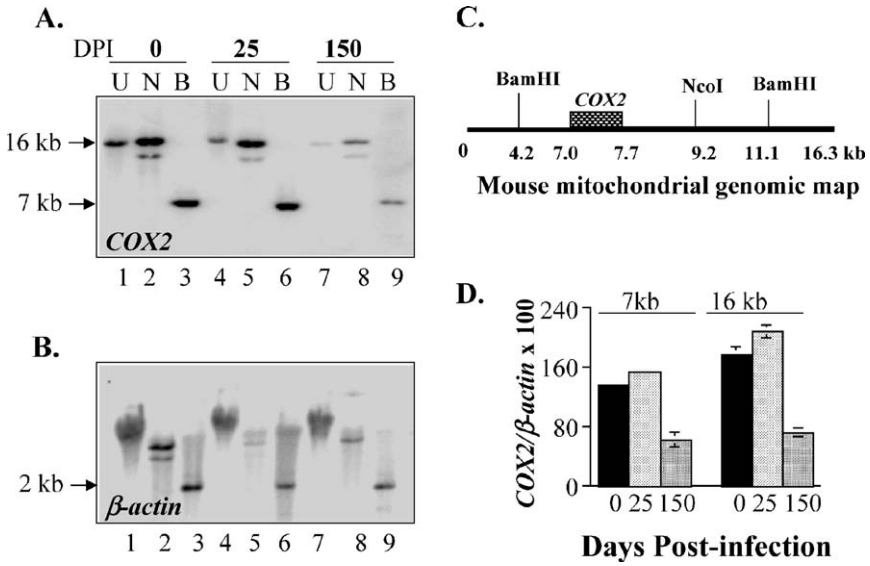

Fig. 3. Southern blot analysis demonstrates a reduction in mtDNA levels in *T. cruzi*-infected murine hearts. C3H/HeN mice were infected with culture-derived *T. cruzi* trypomastigotes (as above). Total DNA was isolated from the cardiac tissue of normal (lanes 1–3) and infected mice sacrificed during acute (25 dpi, lanes 4–6), or chronic (150 dpi, lanes 7–9) phases of infection and disease development, respectively, and resolved by agarose gel electrophoresis. DNA was transferred to nylon membrane and hybridized with [^{32}P] labeled mitochondria-encoded *COX2* probe (A). Membrane was exposed to a phosphorimaging screen for 24 h and the signal captured on a phosphorimager. After stripping the first probe, membrane was hybridized with nuclear-encoded *β-actin* probe (Panel B). (D). Quantitation of mtDNA content in infected murine hearts. The phosphorimages of *COX2* and *β-actin*-hybridized DNA bands were quantitated on a FluorChem 8800 Image Analyzing System. The quantitative data were estimated as the ratio between *COX2*-signal and the corresponding *β-actin* signal × 100. The data present mean values obtained from three independent experiments using heart tissue of at least two mice/experiment. Abbreviations: U, uncut; B, *Bam*HI; N, *Nco*I, and dpi, days post-infection. The position of the *COX2* gene on murine mitochondrial genome is shown (panel C).

infected murine hearts is expressed as the ratio of signal obtained with *COX2* probe to *β-actin* probe (Fig. 3D). The acutely infected murine hearts (25 dpi) exhibited statistically insignificant changes in mtDNA content relative to normal controls (Fig. 3A and D). The level of mtDNA was, however, considerably decreased with progressive disease development in infected mice. Densitometric analysis suggested a 54–60% decline in mtDNA content in chronically infected murine hearts (150 dpi) in comparison to normal controls.

Next, we measured the level of transcripts for mitochondria-encoded respiratory subunits by Northern blot analysis (Fig. 4). The intensity of mitochondria-encoded transcripts was estimated by densitometric analysis and normalized to rRNA (18S and 23S) content. Despite normal levels of mtDNA (Fig. 3A and D), the acutely infected murine hearts exhibited a deficiency of mitochondria-encoded transcripts (Fig. 4). We observed a >50% decrease in mitochondria-encoded CI (*ND1*, *ND2*, and *ND4L*) and CIV (*COX1* and *COX2*) mRNAs in infected murine hearts (25–40 dpi) relative to controls (Fig. 4). The decline in the level of CI- and CIV-transcripts was consistent with the alterations in the enzymatic activity of these complexes at 25–40 dpi (Figs. 1 and 2). In the myocardium of chronically infected mice (150–180 dpi), expression of all of the mitochondria-encoded genes that were examined was significantly reduced (up to 80%) compared to normal controls (Fig. 4B). The repression of the mitochondria-encoded transcripts was consistent with the depletion of mtDNA in chagasic myocardium (Fig. 3). Similar steady-state levels of transcripts for cardiac β-actin and glyceraldehyde phosphate dehydrogenase confirmed the use of similar amounts of RNA for all samples (data not shown).

Considering the substantial repression of the mitochondria-encoded transcripts in infected hearts, we predicted that quantity or assembly of the respiratory complexes might be adversely affected in infected mice. To determine if such is the case, we resolved the RCC on BN gels, quantitated by densitometric analysis, and calculated the intensity of each complex per mg wet tissue weight. As expected, the level of mitochondria-encoded respiratory complexes in infected murine hearts was significantly reduced with disease severity (data not shown). No alterations were observed in molecular size of the respiratory complexes in infected murine hearts relative to controls (Fig. 2B), suggesting that the expression of the mitochondria-encoded genes is essential for the maintenance and assembly of the respiratory chain complexes. The observation of a decline in catalytic staining of the respiratory complexes in infected murine hearts (Fig. 2A) compared to the amount of protein detected by Coomassie (Fig. 2B), however, suggests that the assembled complexes are not enzymatically functional. Together, Southern, Northern, and BN-PAGE analyses have provided evidence for the alteration and repression of the genes encoded by mitochondrial genome and its likely role in assembly and activity of the respiratory complexes during

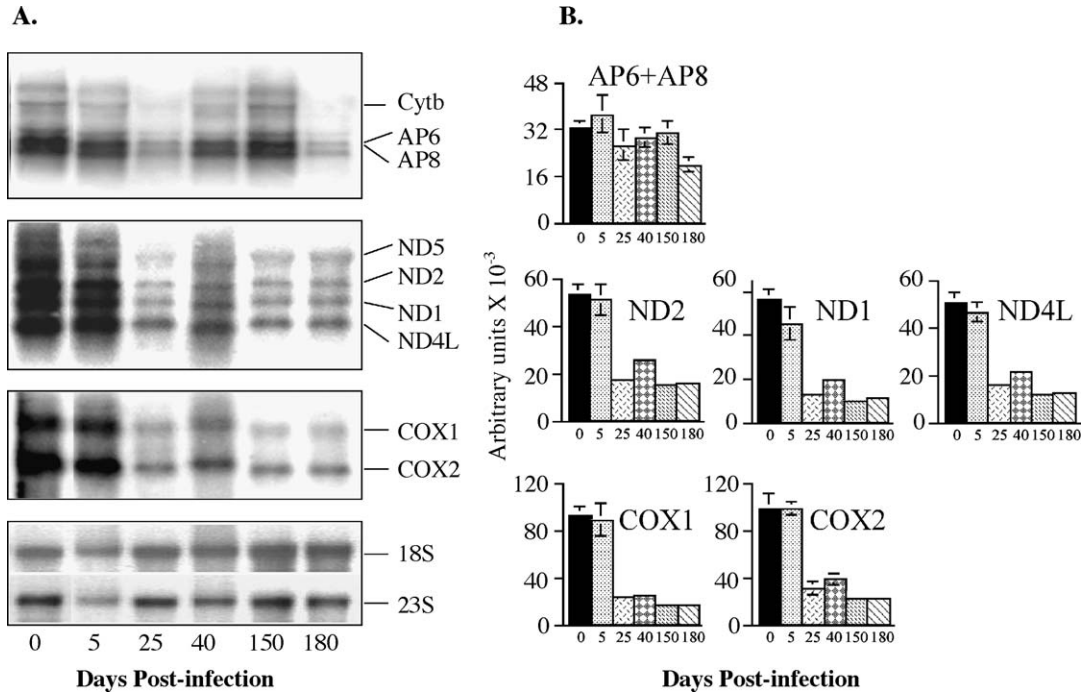

Fig. 4. (A). Northern blot analysis showed the alterations in mitochondria-encoded gene expression in the myocardium of *T. cruzi*-infected mice. Total RNA isolated from whole hearts of normal and infected mice sacrificed at various time-points post-infection was resolved by denaturing agarose gel electrophoresis. RNA was transferred to nylon membrane and hybridized with [^{32}P] labeled, mitochondria-specific *Cytb*, *AP6*, *AP8*, *ND5*, *ND2*, *ND1*, *ND4L*, *COX1*, and *COX2* cDNA probes. (B). Quantitation of mitochondria-encoded transcripts. The phosphorimages of mitochondria-encoded transcripts in normal and infected murine hearts were quantitated by densitometric analysis. The quantitative data were normalized to the amounts of 18S and 23S rRNA and represent the mean values ± S.D. obtained from three independent experiments.

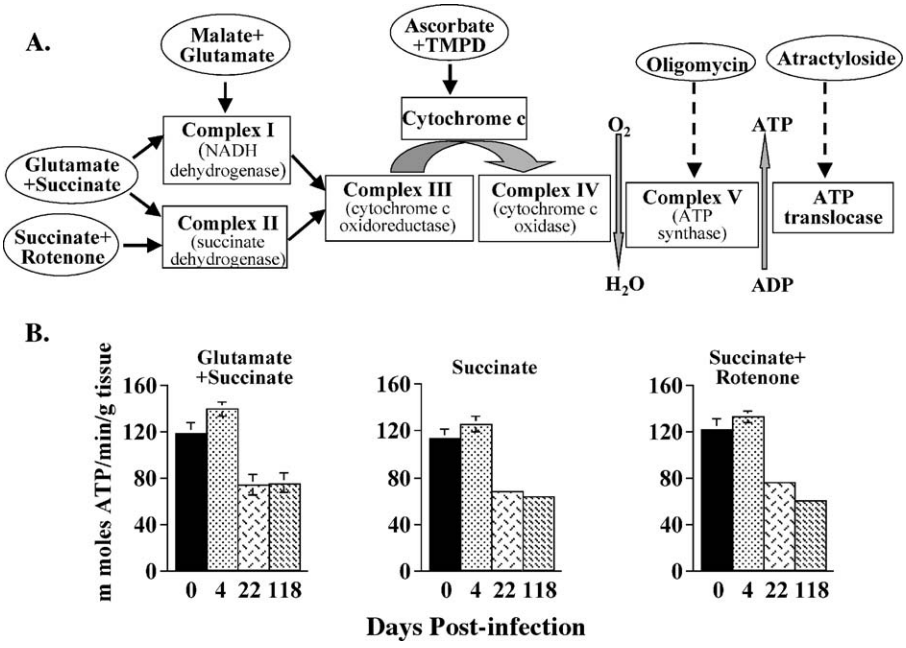

Fig. 5. OXPHOS capacity of the cardiac mitochondria in *T. cruzi*-infected mice. Cardiac mitochondria from normal and infected mice sacrificed at various time-points post-infection were isolated by differential centrifugation and immediately used for OXPHOS-mediated ATP synthesis rates, as described in Materials and methods. Luminescence was recorded for 5 min at 30 s intervals with a 1 s integration time. Data presented as mmol ATP/min/g tissue weight was calculated as mean ± S.D. obtained from triplicate samples (panel B). General schematic representation of mitochondrial respiration including the RCC of the OXPHOS pathway is shown in panel A. Oligomycin and atractyloside (used in this study) inhibit the activity of ATP synthase and ATP translocase, respectively, which are necessary for mitochondrial ATP production.

the course of *T. cruzi* infection and disease development in the myocardium of mice.

3.4. Impaired OXPHOS capacity of the cardiac mitochondria in T. cruzi-infected mice

The ultimate goal of this study was to determine whether the decline in respiratory chain activity affects the cardiac energy status in infected mice. For this, we measured the OXPHOS-mediated ATP synthesis capacity of the cardiac mitochondria in the presence of substrates that donate electrons within the OXPHOS pathway (Fig. 5A). The specificity of ATP synthesis by mitochondria was demonstrated by a ~95% reduction in ATP synthesis upon addition of dinitrophenol (a strong mitochondrial uncoupler) in all experiments irrespective of the substrate used. The residual ATP synthesis (<10%) in the presence of oligomycin and atractyloside, the inhibitors of F_1F_0 ATP synthase and ATP translocase, respectively, was possibly due to the activity of the citric acid cycle and glycolytic pathway.

During the immediate early phase of parasite invasion and infection, the murine myocardium appeared to be fully capable of synthesizing ATP. The ATP production capacity of the cardiac mitochondria harvested at 3–8 dpi was either similar to or higher than that observed in controls with all the substrates examined (Fig. 5B). The acutely infected myocardium (21–45 dpi) showed a 37–40% decrease in mitochondrial ATP production capacity with glutamate + succinate, succinate, and succinate + rotenone substrates relative to controls (Fig. 5B). With progression to the disease phase, the extent of mitochondrial dysfunction was increased. The myocardium of chronic mice sacrificed at >110 dpi exhibited 36% ($P<0.05$), 45% ($P<0.05$), and 50% ($P<0.05$) decline in ATP synthesis capacity, with glutamate + succinate, succinate, and succinate + rotenone substrates, respectively, relative to controls (Fig. 5B). Overall, these data validate the loss in OXPHOS-mediated ATP synthesis capacity of the cardiac mitochondria with progressive disease development in infected mice and suggest that the chagasic hearts might be compromised in terms of energy available for contractile and other metabolic functions.

4. Discussion

The current study is novel in that the molecular and biochemical changes in respiratory complexes and OXPHOS capacity of the chagasic myocardium were evaluated to gain insights into the significance of mitochondrial respiration defects in CCM pathogenesis. Our data clearly show selective inhibition of the respiratory chain complexes in the myocardium of infected mice. The alterations in CI activity were more pronounced during the acute infection phase, CIII and coupled CII + CIII activities were constitutively repressed throughout the infection and disease phase, and the deficiency of CV enzyme appeared during the chronic disease phase (Figs. 1 and 2). The magnitude of decline in respiratory complexes was sufficient to account for the concurrent loss of mitochondrial OXPHOS-mediated ATP synthesis capacity, suggesting energy homeostasis in chagasic myocardium. Various in vitro and in vivo studies indicate that inflammatory intermediates and reactive species, elicited by the host to limit parasite survival [6–9], could cause mitochondria injuries and respiratory chain dysfunction [17–19,33,34]. Additionally, inhibition of CI and CIII complexes can result in increase in free radical generation [34–37]. Our data indicate a plausible mechanism by which *T. cruzi* infection-induced mitochondrial injuries might lead to sustained free radical generation and respiratory dysfunction in CCM.

The current data demonstrating the selective decline in respiratory complexes (Figs. 1 and 2) suggests that reactive radicals contribute to the loss in mitochondrial function. A large body of studies indicates that inflammatory cytokines and reactive intermediates (ROS, RNS) induced to control *T. cruzi* survival in the host [7–9] can also damage host cellular and organelle function [12,13]. Respiratory complexes are particularly sensitive to inhibition [33,34] arising from reactive species-mediated mitochondrial injuries [17–19]. The significance of the current study is that *T. cruzi* infection does not induce unilateral reduction in enzyme activities, but rather specific inactivation of the redox-sensitive CI and CIII complexes. CI and CIII contain prosthetic clusters (4Fe, 4S) that are capable of interacting with reactive species resulting in oxidative damage of the respiratory chain components and enzyme inactivation [36]. The consistent inactivation of CI and CIII complexes in infected murine hearts along with our recent observations indicating increased carbonylation of several subunits of CI, CIII, and CV complexes in the infected myocardium (unpublished data) provides potential mechanism for the rational design of methods to test the contribution of reactive radicals in mitochondrial dysfunction in CCM.

Several studies have previously demonstrated that the mitochondrial respiratory chain is a source of ROS [38,39]. CI and CIII complexes are the prime sites for electron leakage to molecular oxygen resulting in free radical generation in mitochondria [34–37]. The rate of mitochondrial free radical production is inversely proportional to the rate of electron transport, exponentially increasing when CI or CIII complexes of the electron transport chain function at sub optimal level [36]. Our finding of a loss in CI activity in cardiac mitochondria in response to parasite infection (3 dpi) and replication (21–45 dpi) implies that CI might be a potential site of free radical generation in acute mice. Interestingly, consistent deficiencies of CIII activity in the cardiac mitochondria, but not in skeletal muscle mitochondria of the infected mice (unpublished data), suggests CIII as the likely site for sustained free radical generation in the myocardium of infected mice. Future studies aimed at elucidating the events leading to CI and CIII inhibition will indicate strategies to effectively prevent the inactivation of

these complexes and allow the assessment of the role of these complexes in sustained oxidative stress in CCM.

Our data demonstrating the depletion of mtDNA content with progressive disease development in infected myocardium (Fig. 3) provides further support for the free radical hypothesis of mitochondrial dysfunction in CCM. The mitochondrial biogenesis defects leading to a decline in number of mitochondria/cell as well as the mtDNA damage resulting in deletions and/or degradation of DNA can all contribute to a decrease in intact mitochondrial genome. The detection of a similar number of mitochondria in cardiac sections of infected mice exhibiting increasing severity of chronic disease and in normal mice, as determined by transmission electron microscopic analysis [20], suggests that mitochondrial biogenesis defects may not be the probable cause for mtDNA depletion in infected mice. Instead, numerous studies strongly support reactive species to play a prominent role in mtDNA deletions through oxidative damage. mtDNA is highly susceptible to damage by reactive oxidants due to a lack of protective histones [40]. Accumulation of significantly higher levels of DNA oxidation product 8-hydroxydeoxyguanosine in mtDNA compared to nuclear DNA and increased degradation of the mutated mtDNA is shown in a variety of in vitro and in vivo conditions of oxidative stress [41–43]. Given the inhibition of redox-sensitive CI and CIII complexes that are also the prime site for free radical generation in mitochondria, it is reasonable to postulate that ROS-induced alterations resulting in deletions or degradation of oxidatively damaged mtDNA contribute to mtDNA depletion in chagasic myocardium.

The magnitude of the mtDNA defects in chronic myocardium (Fig. 3) was proportional to the quantitative deficiencies of all of the mitochondria-encoded transcripts examined (Fig. 4) and to the loss in the activity of the respiratory complexes (Figs. 1 and 2). These observations suggest that mtDNA defects are at least partially responsible for the respiratory chain dysfunction in chagasic myocardium. This notion is supported by others documenting an intimate link between mtDNA depletion and a decrease in respiratory complexes activities and OXPHOS capacity in failing hearts [44]. Recent studies using cultured neuronal cells or cardiomyocytes have also demonstrated that ROS-mediated mtDNA damage can result in alterations in mitochondria-encoded gene expression and deficiency of mitochondrial respiration [45,46].

The ultimate goal of these studies was to determine the physiological effect of mitochondrial defects on cardiac energy status. The respiratory chain-mediated oxidation of the high-energy carriers (NADH and $FADH_2$) and phosphorylation process provides >90% of the cellular ATP energy for the contractile and other metabolic functions of the heart. A defect in any component of the respiratory chain may compromise OXPHOS capacity and cardiac energy availability. Considering that the inhibition of CI activity in cardiac tissue of the infected mice was equivalent to that detected in skeletal muscle, CI defects may not contribute to altered ATP synthesis efficiency in the myocardium. This is not surprising, as a greater than 85% inhibition of CI in fibroblast cell lines is required before an impairment of mitochondrial respiration was observed [47]. We surmise that inhibition of the CIII and CV activities might be the likely cause for the loss in mitochondria ATP production capacity in the myocardium with progressive CCM. The extent of loss in cardiac mitochondria capacity to produce ATP was increased with disease severity, suggesting energy homeostasis in CCM.

In conclusion, the observations of a selective inhibition of redox-sensitive CI and CIII complexes that are also the site of free radical generation in mitochondria suggest that free radical-mediated oxidative damage contribute to the loss of mitochondria function in the myocardium of chagasic mice. The heart-specific progressive and sustained deficiencies of the respiratory chain activity leading to an overall decline in mitochondrial energy synthesis capacity imply the pathophysiologic significance of the OXPHOS dysfunction in CCM.

Finally, mtDNA base substitution mutations and mtDNA rearrangement due to deletions or insertions have been linked to a variety of heart diseases. An accumulation of the mtDNA deletions in the myocardium is frequently linked to cardiac hypertrophy [48,49], conduction block [50,51], or heart failure [44]. Furthermore, there is now a consensus view that mutations in mtDNA and abnormalities in mt function are associated with ischemic heart disease and dilated cardiomyopathy [52–54]. This study, to our knowledge, is the first to provide evidence for depletion of mtDNA, deficiencies of mitochondria-encoded gene expression, and defects in mitochondrial respiratory chain-associated OXPHOS capacity with CCM development in mice. Future studies could determine whether the impaired mitochondrial tolerance because of oxidative stress result in increased vulnerability of mitochondrial DNA and energetics and thereby constitute a mechanism in myocardial dysfunction in CCM.

Acknowledgements

This work was supported in part by grants from the American Heart Association (0160074Y) and the National Institutes of Health (AI053098-01). Our thanks are due to Dr. Istvan Boldogh for constructive discussion.

References

[1] World Health Organization, Chagas disease: tropical diseases progress in research, 1997–1998, WHO Tech. Rep. Ser. 1 (1999) 1.
[2] A. Rassi Jr., A. Rassi, W.C. Little, Chagas' heart disease, Clin. Cardiol. 23 (2000) 883–889.
[3] L. Zhang, R.L. Tarleton, Parasite persistence correlates with disease

severity and localization in chronic Chagas' disease, J. Infect. Dis. 180 (1999) 480–486.
[4] E. Cunha-Neto, J. Kalil, Heart-infiltrating and peripheral T cells in the pathogenesis of human Chagas' disease cardiomyopathy, Autoimmunity 34 (2001) 187–192.
[5] J.S. Leon, D.M. Engman, Autoimmunity in Chagas heart disease, Int. J. Parasitol. 31 (2001) 555–561.
[6] R.H. Schirmer, T. Schollhammer, G. Eisenbrand, R.L. Krauth-Siegel, Oxidative stress as a defense mechanism against parasitic infections, Free Radic. Res. Commun. 3 (1987) 3–12.
[7] E.C. Lima, I. Garcia, M.H. Vicentelli, P. Vassalli, P. Minoprio, Evidence for a protective role of tumor necrosis factor in the acute phase of *Trypanosoma cruzi* infection in mice, Infect. Immun. 65 (1997) 457–465.
[8] M.A. Munoz-Fernandez, M.A. Fernandez, M. Fresno, Synergism between tumor necrosis factor-alpha and interferon-gamma on macrophage activation for the killing of intracellular *Trypanosoma cruzi* through a nitric oxide-dependent mechanism, Eur. J. Immunol. 22 (1992) 301–307.
[9] R.L. Cardoni, M.I. Antunez, C. Morales, I.R. Nantes, Release of reactive oxygen species by phagocytic cells in response to live parasites in mice infected with *Trypanosoma cruzi*, Am. J. Trop. Med. Hyg. 56 (1997) 329–334.
[10] S.A. Laucella, M.E. Rottenberg, E.H. de Titto, Role of cytokines in resistance and pathology in *Trypanosoma cruzi* infection, Rev. Argent. Microbiol. 28 (1996) 99–109.
[11] R. Perez-Fuentes, J.F. Guegan, C. Barnabe, A. Lopez-Colombo, H. Salgado-Rosas, E. Torres-Rasgado, B. Briones, M. Romero-Diaz, J. Ramos-Jimenez, C. Sanchez-Guillen Mdel, Severity of chronic Chagas disease is associated with cytokine/antioxidant imbalance in chronically infected individuals, Int. J. Parasitol. 33 (2003) 293–299.
[12] J.L. Martindale, N.J. Holbrook, Cellular response to oxidative stress: signaling for suicide and survival, J. Cell. Physiol. 192 (2002) 1–15.
[13] S. Ueda, H. Masutani, H. Nakamura, T. Tanaka, M. Ueno, J. Yodoi, Redox control of cell death, Antioxid. Redox Signal. 4 (2002) 405–414.
[14] K. Bachmaier, N. Neu, C. Pummerer, G.S. Duncan, T.W. Mak, T. Matsuyama, J.M. Penninger, iNOS expression and nitrotyrosine formation in the myocardium in response to inflammation is controlled by the interferon regulatory transcription factor 1, Circulation 96 (1997) 585–591.
[15] G.A. Martins, M.A. Cardoso, J.C. Aliberti, J.S. Silva, Nitric oxide-induced apoptotic cell death in the acute phase of *Trypanosoma cruzi* infection in mice, Immunol. Lett. 63 (1998) 113–120.
[16] H.B. Tanowitz, J.P. Gumprecht, D. Spurr, T.M. Calderon, M.C. Ventura, C. Raventos-Suarez, S. Kellie, S.M. Factor, V.B. Hatcher, M. Wittner, et al., Cytokine gene expression of endothelial cells infected with *Trypanosoma cruzi*, J. Infect. Dis. 166 (1992) 598–603.
[17] H.M. Piper, T. Noll, B. Siegmund, Mitochondrial function in the oxygen depleted and reoxygenated myocardial cell, Cardiovasc. Res. 28 (1994) 1–15.
[18] A.E. Vercesi, A.J. Kowaltowski, M.T. Grijalba, A.R. Meinicke, R.F. Castilho, The role of reactive oxygen species in mitochondrial permeability transition, Biosci. Rep. 17 (1997) 43–52.
[19] S.M. Cardoso, C. Pereira, R. Oliveira, Mitochondrial function is differentially affected upon oxidative stress, Free Radic. Biol. Med. 26 (1999) 3–13.
[20] N. Garg, V.L. Popov, J. Papaconstantinou, Profiling gene transcription reveals a deficiency of mitochondrial oxidative phosphorylation in *Trypanosoma cruzi*-infected murine hearts: implications in chagasic myocarditis development, Biochim. Biophys. Acta 1638 (2003) 106–120.
[21] F. Plata, F. Garcia Pons, H. Eisen, Antigenic polymorphism of *Trypanosoma cruzi*: clonal analysis of trypomastigote surface antigens, Eur. J. Immunol. 14 (1984) 392–399.
[22] D.M. Eble, F.G. Spinale, Contractile and cytoskeletal content, structure, and mRNA levels with tachycardia-induced cardiomyopathy, Am. J. Physiol. 268 (1995) H2426–H2439.
[23] M.A. Bradford, A rapid and sensitive method for quantitation of microgram quantities of protein utilizing the principle of protein-DNA binding, Anal. Biochem. 72 (1976) 248–254.
[24] I.A. Trounce, Y.L. Kim, A.S. Jun, D.C. Wallace, Assessment of mitochondrial oxidative phosphorylation in patient muscle biopsies, lymphoblasts, and transmitochondrial cell lines, Methods Enzymol. 264 (1996) 484–509.
[25] D. Jarreta, J. Orus, A. Barrientos, O. Miro, E. Roig, M. Heras, C.T. Moraes, F. Cardellach, J. Casademont, Mitochondrial function in heart muscle from patients with idiopathic dilated cardiomyopathy, Cardiovasc. Res. 45 (2000) 860–865.
[26] H. Schagger, Native electrophoresis for isolation of mitochondrial oxidative phosphorylation protein complexes, Methods Enzymol. 260 (1995) 190–202.
[27] E. Zerbetto, L. Vergani, F. Dabbeni-Sala, Quantification of muscle mitochondrial oxidative phosphorylation enzymes via histochemical staining of blue native polyacrylamide gels, Electrophoresis 18 (1997) 2059–2064.
[28] P.S. Coelho, A. Klein, A. Talvani, S.F. Coutinho, O. Takeuchi, S. Akira, J.S. Silva, H. Canizzaro, R.T. Gazzinelli, M.M. Teixeira, Glycosylphosphatidylinositol-anchored mucin-like glycoproteins isolated from *Trypanosoma cruzi* trypomastigotes induce in vivo leukocyte recruitment dependent on MCP-1 production by IFN-gamma-primed-macrophages, J. Leukoc. Biol. 71 (2002) 837–844.
[29] P. Chomczynski, N. Sacchi, Single-step method of RNA isolation by acid guanidinium thiocyanate-phenol-chloroform extraction, Anal. Biochem. 162 (1987) 156–159.
[30] B. Wilbourn, D.N. Nesbeth, L.J. Wainwright, M.C. Field, Proteasome and thiol involvement in quality control of glycosylphosphatidylinositol anchor addition, Biochem. J. 332 (1998) 111–118.
[31] R.W. Taylor, M.A. Birch-Machin, K. Bartlett, D.M. Turnbull, Succinate-cytochrome *c* reductase: assessment of its value in the investigation of defects of the respiratory chain, Biochim. Biophys. Acta 1181 (1993) 261–265.
[32] F.N. Gellerich, S. Trumbeckaite, K. Hertel, S. Zierz, U. Muller-Werdan, K. Werdan, H. Redl, G. Schlag, Impaired energy metabolism in hearts of septic baboons: diminished activities of Complex I and Complex II of the mitochondrial respiratory chain, Shock 11 (1999) 336–341.
[33] D.T. Lucas, L.I. Szweda, Declines in mitochondrial respiration during cardiac reperfusion: age-dependent inactivation of alpha-ketoglutarate dehydrogenase, Proc. Natl. Acad. Sci. U. S. A. 96 (1999) 6689–6693.
[34] H.A. Sadek, K.M. Humphries, P.A. Szweda, L.I. Szweda, Selective inactivation of redox-sensitive mitochondrial enzymes during cardiac reperfusion, Arch. Biochem. Biophys. 406 (2002) 222–228.
[35] T. Ide, H. Tsutsui, S. Kinugawa, H. Utsumi, D. Kang, N. Hattori, K. Uchida, K. Arimura, K. Egashira, A. Takeshita, Mitochondrial electron transport complex I is a potential source of oxygen free radicals in the failing myocardium, Circ. Res. 85 (1999) 357–363.
[36] E.J. Lesnefsky, T.I. Gudz, C.T. Migita, M. Ikeda-Saito, M.O. Hassan, P.J. Turkaly, C.L. Hoppel, Ischemic injury to mitochondrial electron transport in the aging heart: damage to the iron–sulfur protein subunit of electron transport complex III, Arch. Biochem. Biophys. 385 (2001) 117–128.
[37] Q. Chen, E.J. Vazquez, S. Moghaddas, C.L. Hoppel, E.J. Lesnefsky, Production of reactive oxygen species by mitochondria: central role of complex III, J. Biol. Chem. 278 (38) (2003) 36027–36031.
[38] D.C. Wallace, Mitochondrial defects in cardiomyopathy and neuromuscular disease, Am. Heart J. 139 (2000) S70–S85.
[39] H. Tsutsui, Oxidative stress in heart failure: the role of mitochondria, Int. Med. 40 (2001) 1177–1182.
[40] Y.H. Wei, C.Y. Lu, H.C. Lee, C.Y. Pang, Y.S. Ma, Oxidative damage and mutation to mitochondrial DNA and age-dependent decline of mitochondrial respiratory function, Ann. N.Y. Acad. Sci. 854 (1998) 155–170.

[41] C.M. Palmeira, J. Serrano, D.W. Kuehl, K.B. Wallace, Preferential oxidation of cardiac mitochondrial DNA following acute intoxication with doxorubicin, Biochim. Biophys. Acta 1321 (1997) 101–106.
[42] M.D. Williams, H. Van Remmen, C.C. Conrad, T.T. Huang, C.J. Epstein, A. Richardson, Increased oxidative damage is correlated to altered mitochondrial function in heterozygous manganese superoxide dismutase knockout mice, J. Biol. Chem. 273 (1998) 28510–28515.
[43] J. Serrano, C.M. Palmeira, D.W. Kuehl, K.B. Wallace, Cardioselective and cumulative oxidation of mitochondrial DNA following subchronic doxorubicin administration, Biochim. Biophys. Acta 1411 (1999) 201–205.
[44] T. Ide, H. Tsutsui, S. Hayashidani, D. Kang, N. Suematsu, K. Nakamura, H. Utsumi, N. Hamasaki, A. Takeshita, Mitochondrial DNA damage and dysfunction associated with oxidative stress in failing hearts after myocardial infarction, Circ. Res. 88 (2001) 529–535.
[45] S.M. de La Monte, J.R. Wands, Mitochondrial DNA damage and impaired mitochondrial function contribute to apoptosis of insulin-stimulated ethanol-exposed neuronal cells, Alcohol Clin. Exp. Res. 25 (2001) 898–906.
[46] N. Suematsu, H. Tsutsui, J. Wen, D. Kang, M. Ikeuchi, T. Ide, S. Hayashidani, T. Shiomi, T. Kubota, N. Hamasaki, A. Takeshita, Oxidative stress mediates tumor necrosis factor-alpha-induced mitochondrial DNA damage and dysfunction in cardiac myocytes, Circulation 107 (2003) 1418–1423.
[47] A.M. James, Y.H. Wei, C.Y. Pang, M.P. Murphy, Altered mitochondrial function in fibroblasts containing MELAS or MERRF mitochondrial DNA mutations, Biochem. J. 318 (Pt 2) (1996) 401–407.
[48] T. Tokoro, H. Ito, T. Suzuki, Alterations in mitochondrial DNA and enzyme activities in hypertrophied myocardium of stroke-prone SHRS, Clin. Exp. Hypertens. 18 (1996) 595–606.
[49] T. Arai, K. Nakahara, H. Matsuoka, M. Sawabe, K. Chida, S. Matsushita, K. Takubo, N. Honma, K. Nakamura, N. Izumiyama, Y. Esaki, Age-related mitochondrial DNA deletion in human heart: its relationship with cardiovascular diseases, Aging Clin. Exp. Res. 15 (2003) 1–5.
[50] W. Sato, M. Tanaka, S. Sugiyama, K. Hattori, T. Ito, H. Kawaguchi, H. Onozuka, H. Yasuda, K. Ito, G. Takada, et al., Deletion of mitochondrial DNA in a patient with conduction block, Am. Heart J. 125 (1993) 550–552.
[51] K.H. Katsanos, C.J. Pappas, D. Patsouras, L.K. Michalis, G. Kitsios, M. Elisaf, E.V. Tsianos, Alarming atrioventricular block and mitral valve prolapse in the Kearns–Sayre syndrome, Int. J. Cardiol. 83 (2002) 179–181.
[52] J. Marin-Garcia, M.J. Goldenthal, R. Ananthakrishnan, D. Mirvis, Specific mitochondrial DNA deletions in canine myocardial ischemia, Biochem. Mol. Biol. Int. 40 (1996) 1057–1065.
[53] N. Takeda, Cardiomyopathies and mitochondrial DNA mutations, Mol. Cell. Biochem. 176 (1997) 287–290.
[54] Z. Zeng, Z. Zhang, H. Yu, M.J. Corbley, Z. Tang, T. Tong, Mitochondrial DNA deletions are associated with ischemia and aging in Balb/c mouse brain, J. Cell. Biochem. 73 (1999) 545–553.